ChemPubSoc Europe

DOI: 10.1002/cssc.201601081

CHEMSUSCHEM Communications

Electrochemical Dealloying of $PdCu_3$ Nanoparticles to Achieve Pt-like Activity for the Hydrogen Evolution Reaction

Rajkumar Jana,[a] Anupam Bhim,[a] Pallavi Bothra,[a] Swapan K. Pati,[a, b] and Sebastian C. Peter*[a]

Manipulating the d-band center of the metal surface and hence optimizing the free energy of hydrogen adsorption (ΔG_H) close to the optimal adsorption energy ($\Delta G_H = 0$) for hydrogen evolution reaction (HER), is an efficient strategy to enhance the activity for HER. Herein, we report a oleylamine-mediated (acting as the solvent, stabilizer, and reducing agent) strategy to synthesize intermetallic $PdCu_3$ nanoparticles (NPs) without using any external reducing agent. Upon electrochemical cycling, $PdCu_3$ transforms into Pd-rich PdCu ($\Delta G_H =$ 0.05 eV), exhibiting remarkably enhanced activity (with a current density of 25 mA cm^{-2} at ~69 mV overpotential) as an alternative to Pt for HER. The first-principle calculation suggests that formation of low coordination number Pd active sites alters the d-band center and hence optimal adsorption of hydrogen, leading to enhanced activity. This finding may provide guidelines towards the design and development of Pt-free highly active and robust electrocatalysts.

In recent years, hydrogen generation has become an enormous interest owing to its application in clean energy technologies, such as fuel cells and solar fuel generators.[1] Despite its high cost and scarcity, platinum-based catalysts are the most effective catalysts for electrochemical HER owing to their low overpotentials and fast reduction kinetics in acidic medium.[2] In search of non-Pt-based catalysts, transition metal (Mo, W, Ni, Pd, and Cu) based phosphides, carbides, nitrides, sulfides, selenides, and bimetallic systems have been proposed as efficient catalysts for HER.[2a, 3] Especially, transition metal sulfides (e.g., MoS_2,[4] CoS_2,[5] and WS_2[6]), phosphides (e.g., Ni_5P_4-Ni_2P nanosheets,[7] CoP,[8] and Cu_3P[9]), and phosphosulphides (e.g., CoPS,[10] MoPS,[11] and PdPS[3b]), as well as carbide systems (e.g., Mo_2C[12] and WC[13]), have been recently identified as the most promising HER electrocatalysts. Despite promising activity and stability, these catalysts are far beyond the Pt-based ones with high overpotentials and less exchange current density.[2a] Therefore, development of non-Pt-based catalysts that are superior or comparable to Pt is still desperately needed for the successful application of water splitting for hydrogen generation. Based on the "Volcano Plot", which relates the enthalpy of hydrogen adsorption and consequent electroneutrality for free energy of adsorption, Pd is considered to be a highly efficient hydrogen evolution catalyst comparable to Pt.[14] Though Pd is highly active for hydrogen evolution, it enhances the hydrogen solubility under appropriate temperature and pressure, which leads to the formation of hydride phases and lattice expansion causing instability.[15] Formation of hydride can be suppressed to a large extent by alloying of Pd with other metals.[16] On the other hand, in comparison with other inexpensive metals (e.g., Ni, Co, and Mo), Cu is low cost and highly abundant. Recently, Cu-based catalysts have shown considerable activities towards HER both in acidic/basic and neutral medium.[3c, 7, 17]

In the present study, we report a new catalyst derived from electrochemical dealloying of $PdCu_3$ intermetallic NPs for highly efficient electrochemical HER. To prepare monodisperse $PdCu_3$ intermetallic NPs, a new facile solvothermal method was adopted by co-reducing $Pd(acac)_2$ and $Cu(acac)_2$ in oleylamine at 180 °C. Here, oleylamine was used as the solvent, stabilizer, and reducing agent (see the Supporting Information for complete experimental details). Owing to a large reduction potential difference between Pd^{II}/Pd (+0.915 V)[18] and Cu^{II}/Cu (0.34 V)[19] pairs, it is very unlikely to form intermetallic $PdCu_3$ without the use of a strong external reducing agent. However, the presence of cetyl trimethylammonium bromide (CTAB) controls the reduction rates of Pd and Cu species for facilitating the co-reduction process.[19] The formation of single phase $PdCu_3$ in cubic symmetry has been confirmed by powder XRD (Figures 1a and S1 in the Supporting Information). The XPS spectrum of $PdCu_3$ NPs shown in Figure 1b exhibits peaks at 335.5 and 340.5 eV, corresponding to Pd $3d_{5/2}$ and Pd $3d_{3/2}$ core levels, while the peaks at 932.5 and 952 eV correspond to Cu $2p_{3/2}$ and Cu $2p_{1/2}$, respectively.[20] The core level XPS spectra clearly indicate the presence of Pd^0 and Cu^0 in the synthesized $PdCu_3$ NPs.[20]

Figure 2a,b shows TEM images of the as-synthesized spherical $PdCu_3$ NPs with an average diameter of 10 nm. The corresponding selected area diffraction (SAED) pattern (Figure 2c) contains (111), (200), (300), (311) crystallographic planes of $PdCu_3$ NPs. The high- resolution TEM (HRTEM) image (Figure 2d) shows the lattice fringes of d-spacing 0.217 nm, which

[a] R. Jana, A. Bhim, Dr. P. Bothra, Prof. S. K. Pati, Dr. S. C. Peter
New Chemistry Unit
Jawaharlal Nehru Centre for Advanced Scientific Research
Jakkur P.O., Bangalore (India)
E-mail: sebastiancp@jncasr.ac.in

[b] Prof. S. K. Pati
Theoretical Sciences Unit
Jawaharlal Nehru Centre for Advanced Scientific Research
Jakkur P.O., Bangalore (India)

Supporting Information and the ORCID identification number(s) for the author(s) of this article can be found under http://dx.doi.org/10.1002/cssc.201601081.

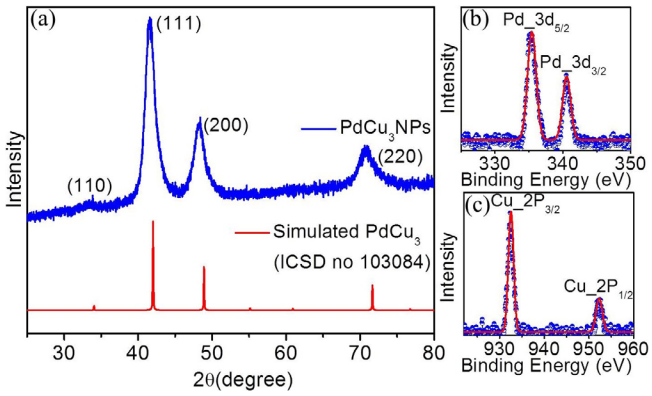

Figure 1. (a) Powder XRD pattern of $PdCu_3$ NPs with respect to the simulated pattern.[21] High resolution XPS spectra of (b) Pd 3d and (c) Cu 2p core levels of the sample $PdCu_3$ NPs.

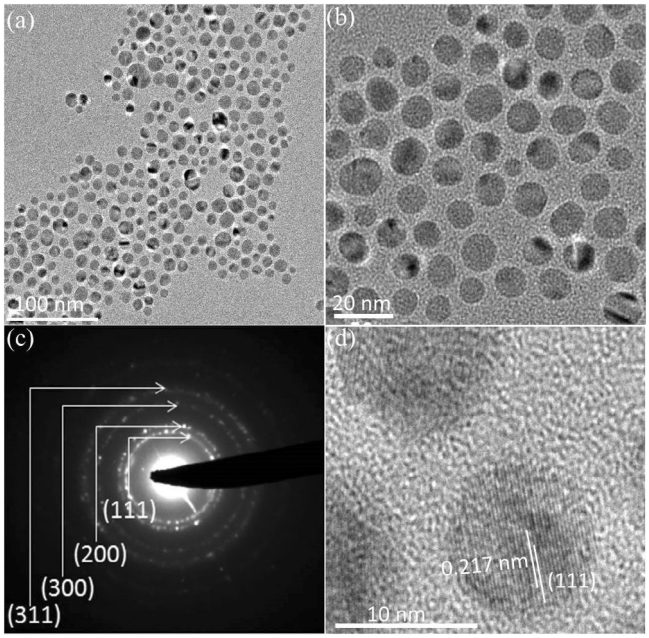

Figure 2. (a–b) TEM images and (c) SAED pattern of the as-synthesized $PdCu_3$ NPs, and (d) HRTEM image of a single $PdCu_3$ NP.

corresponds to the (111) plane of the cubic intermetallic $PdCu_3$ NPs. SAED pattern and d-spacing value calculated from HRTEM clearly confirm the formation of $PdCu_3$ NPs. A high-angle annular dark field scanning TEM (HAADF-STEM) image, and selected area elemental mapping show that Pd (yellow) and Cu (red) elements are uniformly distributed throughout nanoparticles (Figure S2). Energy-dispersive X-ray spectroscopy (EDS) data taken on an ensemble of nanoparticles (Figure S3 a, b) shows the presence of Pd and Cu elements with atomic percentage of 26.74 and 73.26 at%, respectively, which is in good agreement with the expected stoichiometric ratio of 1:3 for $PdCu_3$. This result is further supported by point EDS on a single nanoparticle and inductively coupled plasma atomic-emission spectroscopy (ICP-AES) analysis (Figure S4 a, b and Table S1).

HER catalyzed by $PdCu_3$ NPs have been investigated in 0.5 M H_2SO_4 solution using a three-electrode setup with Pt wire and Ag/AgCl as the counter and reference electrodes, respectively. All the potentials have been calibrated versus the reversible hydrogen electrode (RHE). Commercial Pt/C (40 wt%, Alfa Aesar) and Pd/C (40 wt%) synthesized experimentally using the same conditions have been used to compare catalytic performance (Figure S5). Figure 3 a and b show the polarization curves of different catalysts where activities of different catalysts are compared. Figure 3 a shows a dramatic enhancement of the HER activity of $PdCu_3$ after continuous potential cycling from 0.391 to 0.941 V (vs. RHE). The onset potential as well as overpotential at 10 mA cm^{-2} (η_{10}) and 20 mA cm^{-2} (η_{20}) shift positively with the increased number of potential cycles reaching a maximum value after 1000 cycles. The onset potential observed for $PdCu_3$ NPs is −100 mV versus RHE with η_{10} and

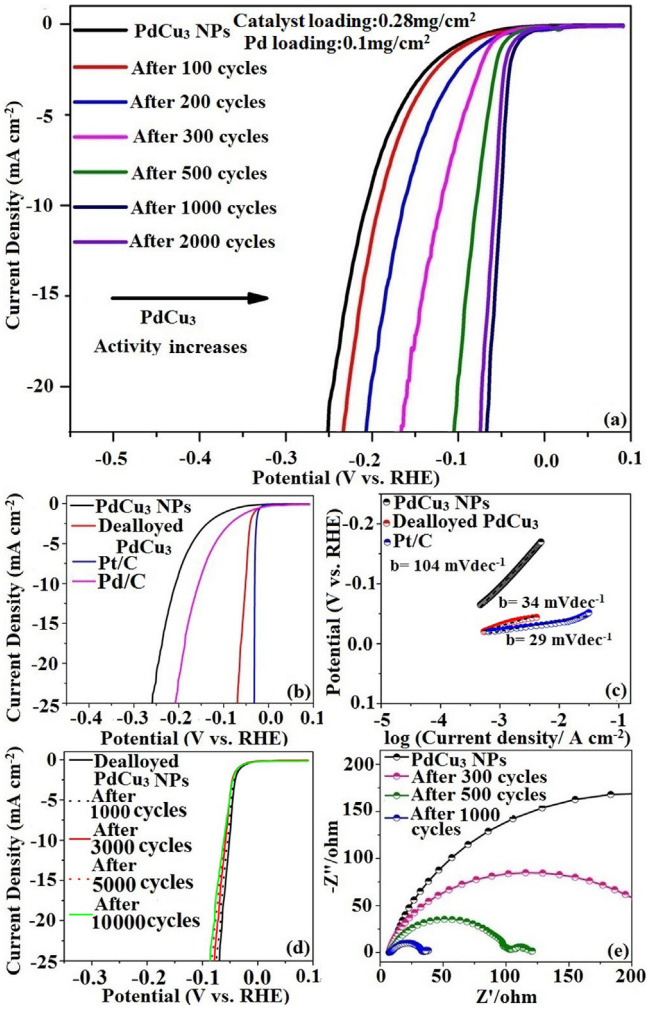

Figure 3. (a) Linear sweep voltammograms (LSVs) of $PdCu_3$ NPs in 0.5 M H_2SO_4 before and after cycling tests. (b) LSVs of $PdCu_3$, dealloyed $PdCu_3$, commercial Pt/C (40 wt%), and synthesized Pd/C (40 wt%) in 0.5 M H_2SO_4; scan rate = 1 mV s^{-1}. (c) Tafel plots for $PdCu_3$, dealloyed $PdCu_3$, and commercial Pt/C (40 wt%) in 0.5 M H_2SO_4. (d) LSVs of dealloyed $PdCu_3$ catalysts before and after 1000, 3000, and 5000 cycles. (e) Nyquist plots of $PdCu_3$ NPs and electrochemically dealloyed $PdCu_3$ NPs. AC data obtained at −0.08 V vs. RHE with 5 mV AC amplitude in 0.5 M H_2SO_4. The frequency range used for the impedance measurement was 100 kHz to 10 mHz.

η_{20} value at −210 and −250 mV respectively for a catalyst mass loading of 0.28 mg cm^{-2} (Pd loading: 0.1 mg cm^{-2}). However, the catalyst obtained after 1000 potential cycles shows much reduced HER onset potential (−10 mV) as well as η_{10} (−50 mV) and η_{20} (−63 mV), which is almost equivalent to the current state-of-the-art material Pt/C (Figure 3b).

Comparison of the present data with the literature is difficult as the mass loading are not the same. However, under similar conditions (without considering similar mass loading for all the catalysts), these potential values are better than that of the other acid-stable non-Pt-based HER electrocatalysts, including PdPS [onset potential (η_{onset}) ≈ −50 mV; η_{10} ≈ −90 mV],[3b] $Pd_{17}Se_{15}$ (η_{onset} ≈ −80 mV; η_{10} ≈ −182 mV),[22] Pd_7Se_4 (η_{onset} ≈ −70 mV; η_{10} ≈ −162 mV),[22] Pd_4Se (η_{onset} ≈ −30 mV; η_{10} ≈ −94 mV),[22] Pd_2Si (η_{10} ≈ −192 mV),[23] exfoliated MoS_2 (η_{10} ≈ −187 mV),[4] WS_2 (η_{onset} ≈ −100 mV),[6] CoS_2/RGO-CNT composites (η_{10} ≈ −142 mV),[5] Ni_5P_4-Ni_2P nanosheets (η_{onset} ≈ −54 mV; η_{10} ≈ −120 mV),[7] CoP (η_{20} ≈ −95 mV),[8] Cu_3P nanowires (η_{onset} ≈ −62 mV; η_{10} ≈ −143 mV),[9] MoPS (η_{10} ≈ −86 mV)[11] and β-Mo_2C nanotubes (η_{onset} ≈ −82 mV; η_{10} ≈ −172 mV)[12] (Table S2). Though the effect of oleylamine on electrochemical HER and its fate during this process is not known in the literature, it is well-established that presence of nitrogen on the catalyst surface in the form of doped atoms enhances the HER activity.[24] It is well-known that the presence of donor nitrogen atoms on the catalyst surface (either from oleylamine or some other nitrogen-containing solvent) of Pt and Pd enhances the electrocatalytic activity towards the oxygen reduction reaction owing to either a shift of d-band center due to charge transfer or preventing the spectator ions (SO_4^{2-}) from blocking the active sites.[25] Based on the above-mentioned fact, it can be proposed that the presence of nitrogen atoms on the catalyst surface in the form of oleylamine capping is expected to enhance the HER activity of the catalyst and it is expected to be intact on the NP surface upon electrochemical dealloying process.

The catalyst obtained after 1000 cycles on $PdCu_3$ NPs was analyzed by EDS elemental analysis (Figure S2c,d), which shows the atomic percentage of Pd and Cu elements are 42.75 and 57.25 at%, respectively. This composition of the dealloyed catalyst is also well-supported by point EDS on a single NP and ICP-AES data (Figure S4c,d and Table S1). This decrease in atomic percentage of Cu clearly indicates the dissolution of Cu and the formation of relatively more Pd-rich $PdCu_{3-x}$ alloy (approximately $PdCu_{1.3}$), which is commonly observed in Cu-based alloys.[26] The Cu-dissolution phenomenon from $PdCu_3$ intermetallic nanoparticles can be well-understood from the cyclic voltammetry curves in the potential cycling region (0.391–0.941 V vs. RHE). As shown in Figure S6, the intensity of the Cu dissolution peak (0.46–0.625 V vs. RHE in the forward scan) decreases gradually with the increasing number of potential cycles, indicating Cu dissolution from $PdCu_3$ NPs. The Cu etching from $PdCu_3$ NPs was further confirmed by HRTEM image (Figure S7) and elemental mapping (Figure S8). The distance between two lattice fringes (d-spacing) was calculated to be 0.226 nm whereas for (111) plane of $PdCu_3$ NPs is 0.217 nm. This increase in d-spacing clearly indicates the deficiency of Cu in the $PdCu_3$ system and supports the Cu dissolution phenomenon. Elemental mapping (as shown in Figure S8) of the catalyst obtained after 1000 cycles clearly shows that Pd still spreads across the whole NP, but Cu is concentrated in only a few regions of the NP, which indicates that after potential cycling, Cu is etched out from $PdCu_3$ NPs and Pd rich $PdCu_{3-x}$ NPs are formed. No traces of Pt were found through ICP-AES, SEM-EDS, and point EDS (on a single particle) analysis. Additionally, use of carbon as a counter electrode does not change the characteristics activation owing to the dealloying effect (Figure S9), which confirms that any residual Pt from counter electrode is not responsible for the observed activity.

In general, the HER on the catalyst surface can be described either by the Volmer–Heyrovsky mechanism ($H_3O^+ + e^- = H_{ads} + H_2O$ and $H_{ads} + H_3O^+ + e^- = H_2 + H_2O$) and/or Volmer–Tafel mechanism ($H_3O^+ + e^- = H_{ads} + H_2O$ and $H_{ads} + H_{ads} = H_2$).[2a,3f,27] Tafel slope is often used to study the rate determining step of the HER.[3f,27a] A HER following the Volmer–Heyrovsky mechanism leads to a Tafel slope of 120 mV dec^{-1}, while that for Volmer–Tafel mechanism is 30 mV dec^{-1}. In the present study (as shown in Figure 3c), dealloyed $PdCu_3$ shows the value of 34 mV dec^{-1}, which is very close to Pt/C (29 mV dec^{-1}) under identical reaction conditions.[3b] Hence, change in Tafel slope clearly indicates the change in HER mechanism on the catalyst surface; that is, HER on the as-synthesized $PdCu_3$ follows the Volmer–Heyrovsky mechanism, whereas on the dealloyed catalyst it follows the Volmer–Tafel mechanism. The obtained Tafel slope for the dealloyed catalyst is smaller than many highly efficient non-Pt-based HER electrocatalysts, such as $Pd_{17}Se_{15}$(57 mV dec^{-1}),[22] Pd_7Se_4 (56 mV dec^{-1}),[22] Pd_4Se (50 mV dec^{-1}),[22] PdPS (46 mV dec^{-1}),[3b] Pd_2Si (131 mV dec^{-1}),[23] exfoliated MoS_2 (43 mV dec^{-1}),[4] WS_2 (48 mV dec^{-1}),[6] CoP (50 mV dec^{-1}),[8] Cu_3P nanowires (50 mV dec^{-1}),[9] Ni_5P_4-Ni_2P nanosheets (79.1 mV dec^{-1}),[7] CoPS (48 mV dec^{-1})[10] and β-Mo_2C (62 mV dec^{-1})[12] (Table S2). The exchange current density of dealloyed $PdCu_3$ is found to be 1.8×10^{-4} A cm^{-2}.

Further, AC impedance spectroscopic data shows the charge-transfer resistance (R_{CT}, obtained from the diameter of the semicircle of the Nyquist Plot) being low for the dealloyed catalysts (obtained after different cycles), indicating faster kinetics of HER on dealloyed catalysts reaching a lowest R_{CT} value (26 Ω) for the catalysts obtained after 1000 cycles (Figure 3e). Cu-rich intermetallic NPs are considered to be of great interest as electrocatalysis and it was suggested that selective electrochemical dissolution of Cu favors the formation of highly active catalysts.[19,26a,28] Xia et al. reported that upon potential cycling, Cu-rich $PtCu_3$ transforms into highly active Pt-rich electrocatalysts and enhanced electrocatalytic activity was observed.[19] Recently, Lv et al. showed remarkable enhancement in the HER activity of NiAu alloy upon potential cycling.[2a] Lowering of Au coordination number upon dissolution of Ni enhances the HER activity to a large extent, like Pt. A similar effect has been observed in the present study, dissolution of Cu favored the formation of a Pd-rich compound with enhanced electrochemical activity towards HER. During gas evolution on the electrode surface, stability of the electrocatalysts is a major issue. McKone et al. reported that Ni–Mo nanopow-

der, which is considered as one of the best catalysts for HER, degrades during continuous operation.[29] On the other hand, here, the dealloyed $PdCu_3$ catalyst is not only highly active, but also durable to HER. The dealloyed catalyst is cycled between 0.341 and −0.409 V (vs. RHE) at a scan rate of 100 mV s^{-1} for up to 10000 cycles. As shown in Figure 3d, there is nearly no activity change for the dealloyed $PdCu_3$ catalyst, indicating that it is highly durable for HER in 0.5 M H_2SO_4. The stability of the catalyst was further confirmed by TEM analysis (Figure S10). From the HRTEM image (Figure S10b), it can be observed that there is almost no change in d-spacing of the electrode material after 5000 cycles of stability test. This indicates that the dealloyed $PdCu_3$ catalyst is stable even after a large number of potential cycles.

Electronic structure calculations offer the possibility of giving a detailed molecular-level picture of the process involved. Hence, to gain insight into the electrocatalytic activity of $PdCu_3$ (111) towards HER, we have carried out first-principles calculations. As the reaction proceeds through hydrogen atoms adsorbed at the electrode surface (H_{ads}), the rate of the overall reaction is eventually influenced by the free energy of hydrogen adsorption (ΔG_H) considered as single catalytic descriptor. If the binding strength of the hydrogen to the surface is very weak, the adsorption step would limit the overall reaction rate. On the other hand, when the hydrogen binds to the surface very strongly, the desorption step would limit the overall reaction rate. Therefore, it can be inferred that optimal catalysts for HER should have hydrogen adsorption energies close to $\Delta G_H = 0$ eV (i.e., binding energy of hydrogen is neither too weak nor too strong). In the first-principles calculations, surface Pd sites have been considered as catalytically active centers for H adsorption. Each surface of Pd atom(s) in the intermetallic $PdCu_3$ (111) system are surrounded by 9 Cu atoms; hence, the maximum coordination number (n) of surface Pd atom is equal to 9. However, according to the experimental finding, Cu atoms get successively etched out from the $PdCu_3$ (111) surface during the course of electrochemical cycling. Hence, it can be expected that there would be development of structural defects owing to Cu vacancies adjacent to the Pd atom on the $PdCu_3$ (111) surface. This results in the lowering of n of surface Pd atoms in comparison to a perfect surface with the progress of the reaction. To find out the effect of dealloying on catalytic activity, we have calculated ΔG_H as a function of reduction with respect to n of surface Pd atom.

More specifically, neighboring Cu atoms of surface Pd were consecutively removed to create under-coordinated catalytically active Pd sites, and overall six $PdCu_3$ (111) surfaces with n ranging from 9 to 4 were considered (Figure 4a, I–VI) in the present study. From the free energy diagram, it is evident that there is monotonous decline in ΔG_H value with lowering n (Figure 4b).

However, our computational study recommends that at $n = 5$, the catalytic activity of $PdCu_3$ (111) surface should be most favorable with $\Delta G_H = 0.05$ eV, which is very close to the binding energy of optimal HER catalyst ($\Delta G_H = 0$ eV), although still weaker hydrogen absorption compared to Pt with a positive binding energy. Interestingly, as we move to lower n (i.e, $n = 4$)

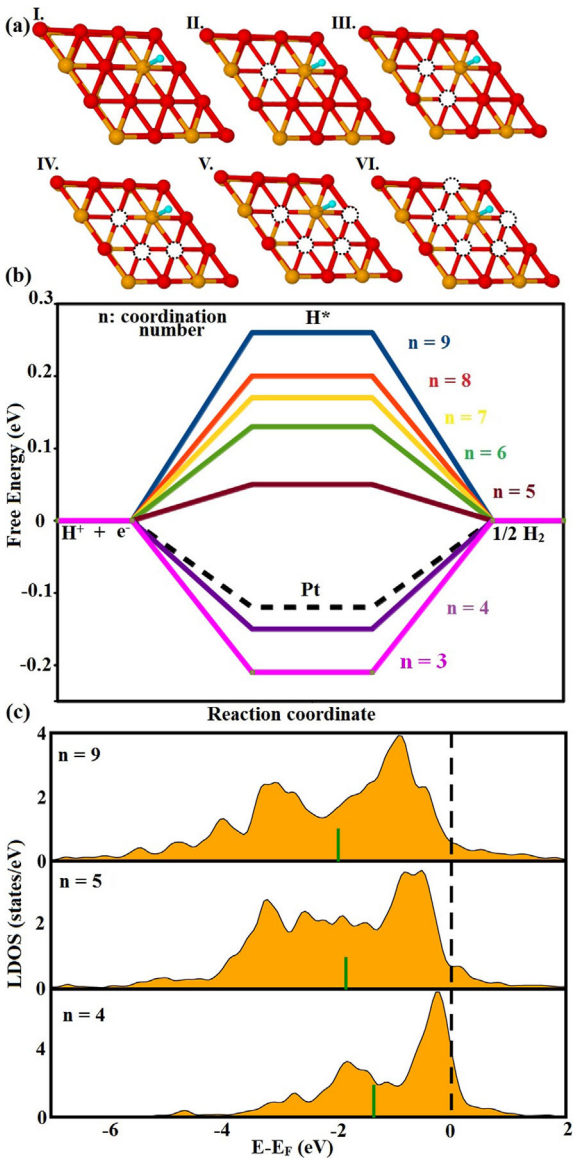

Figure 4. (a) $PdCu_3$ (111) surfaces with $n = 9$–4 (I–VI, respectively). The vacant sites are denoted by the white circles with black dotted boundary. Cu, Pd, and H atoms are represented by red, orange, and cyan colored balls, respectively. (b) Free energy diagram for HER ($U = 0$ V) at Pd sites with varying coordination number ($n = 9$–4). The broken line corresponds to a pure Pt (111) surface. (c) LDOS on Pd atom with $n = 9$, 5, and 4. The Fermi energy (E_F) is represented by a black vertical dashed line. The green thick bar represents the d-band center (E_d) on the Pd atoms of $PdCu_3$ (111) surfaces.

ΔG_H surpasses the optimal value and the H atom strongly adsorbs to the surface with negative binding energy. It can be analyzed through the Sabatier principle, which accounts for optimal surfaces as ones that exhibit moderate binding energies of adsorbates as found for the $n = 5$ system here. This result is in excellent agreement with the experimental findings of enhanced HER activity with lower n during electrochemical cycling. Moreover, it has been experimentally observed that there is a slight decrease in the HER activity after a certain electrochemical cycle (2000 cycles) with respect to pure Pt metal that nicely corroborates with the diminished activity of $PdCu_3$ (111) with $n = 4$. Nevertheless, it should be noted that

the ΔG_H value at $n=5$ (0.05 eV) is far better and that only at $n=4$ (−0.15 eV), the ΔG_H is very close to that of pure Pt metal (−0.12 eV) suggesting insignificant difference in the catalytic activity of pure Pt and $PdCu_3$ (111) ($n=4$) towards HER.

Furthermore, we have calculated the local density of states (LDOS) projected onto three representative surface Pd sites of $PdCu_3$ (111) with $n=9$, 5, and 4 (Figure 4c). The results can be explained using a d-band model because the d-band center is correlated to the adsorption energy of the adsorbate.[30] The calculated d-band centers for the $PdCu_3$ (111) surface with $n=$ 9, 5, and 4 are −2.00, −1.88, and −1.52 eV, respectively. It is well-known that the higher the d-band energy is, stronger the adsorption.[31] It is evident from Figure 4c that as n reduces from 9 to 5 and 4, the d-band center shifts towards the Fermi energy, which suggests stronger adsorption of H to the surface and lowering of ΔG_H. Hence, in the present case, d-band center explains the origin of the enhanced HER activity with reducing the n of Pd.

In summary, we have investigated the effect of dealloying the $PdCu_3$ electrocatalyst, synthesized using oleylamine at 180 °C, on electrochemical HER. Subject to potential cycling between 0.39 and 0.94 V (vs. RHE) in 0.5 M H_2SO_4, $PdCu_3$ NPs transform to a Cu-deficient $PdCu_3$ alloy owing to selective electrochemical dissolution of Cu. The relatively Pd-rich dealloyed $PdCu_3$ NPs show remarkable enhancement in the HER activity almost equivalent to Pt. The dealloyed catalyst is found to be highly stable for a large number of potential cycles. The first principles calculations suggest that enhancement in the catalytic activity for HER arises as a result of the formation of active Pd sites with low coordination number. This dealloyed $PdCu_3$ catalyst can be a promising alternative to Pt in HER for important energy applications. This present study can be extended to synthesize other Pd-based first-row transition metal alloys for HER catalytic tuning and optimization, which in turn will help to develop non-Pt-based highly active and stable catalysts for HER.

Acknowledgements

Financial support from the Department of Science and Technology (DST) (Grant SB/FT/CS-07/2011), Sheikh Saqr Laboratory and Jawaharlal Nehru Centre for Advanced Scientific Research (JNCASR) is gratefully acknowledged. R. K. J. and P. B. thank Council of Scientific and Industrial Research, JNCASR and DST for research fellowship, A.B. thanks JNCASR for summer student research fellowship, S. K. P. thanks DST for J. C. Bose fellowship and S. C. P. thanks DST for Ramanujan fellowship (Grant SR/S2/RJN-24/2010). We are grateful to Prof. C. N. R. Rao for his constant support and encouragement.

Keywords: electrochemical dealloying · hydrogen absorption · hydrogen evolution reaction · nanoparticles · platinum-free catalyst

[1] a) D. V. Esposito, S. T. Hunt, A. L. Stottlemyer, K. D. Dobson, B. E. McCandless, R. W. Birkmire, J. G. Chen, *Angew. Chem. Int. Ed.* **2010**, *49*, 9859 – 9862; *Angew. Chem.* **2010**, *122*, 10055 – 10058; b) H. B. Gray, *Nat. Chem.* **2009**, *1*, 7; c) N. S. Lewis, D. G. Nocera, *Proc. Natl. Acad. Sci. USA* **2006**, *103*, 15729 – 15735.

[2] a) H. Lv, Z. Xi, Z. Chen, S. Guo, Y. Yu, W. Zhu, Q. Li, X. Zhang, M. Pan, G. Lu, *J. Am. Chem. Soc.* **2015**, *137*, 5859 – 5862; b) J. R. McKone, E. L. Warren, M. J. Bierman, S. W. Boettcher, B. S. Brunschwig, N. S. Lewis, H. B. Gray, *Energy Environ. Sci.* **2011**, *4*, 3573 – 3583.

[3] a) J. M. McEnaney, J. C. Crompton, J. F. Callejas, E. J. Popczun, C. G. Read, N. S. Lewis, R. E. Schaak, *Chem. Commun.* **2014**, *50*, 11026 – 11028; b) S. Sarkar, S. Sampath, *Chem. Commun.* **2014**, *50*, 7359 – 7362; c) X. Liu, S. Cui, Z. Sun, P. Du, *Chem. Commun.* **2015**, *51*, 12954 – 12957; d) P. D. Tran, M. Nguyen, S. S. Pramana, A. Bhattacharjee, S. Y. Chiam, J. Fize, M. J. Field, V. Artero, L. H. Wong, J. Loo, *Energy Environ. Sci.* **2012**, *5*, 8912 – 8916; e) W.-F. Chen, J. T. Muckerman, E. Fujita, *Chem. Commun.* **2013**, *49*, 8896 – 8909; f) Y. Li, H. Wang, L. Xie, Y. Liang, G. Hong, H. Dai, *J. Am. Chem. Soc.* **2011**, *133*, 7296 – 7299.

[4] M. A. Lukowski, A. S. Daniel, F. Meng, A. Forticaux, L. Li, S. Jin, *J. Am. Chem. Soc.* **2013**, *135*, 10274 – 10277.

[5] S. Peng, L. Li, X. Han, W. Sun, M. Srinivasan, S. G. Mhaisalkar, F. Cheng, Q. Yan, J. Chen, S. Ramakrishna, *Angew. Chem.* **2014**, *126*, 12802 – 12807.

[6] L. Cheng, W. Huang, Q. Gong, C. Liu, Z. Liu, Y. Li, H. Dai, *Angew. Chem. Int. Ed.* **2014**, *53*, 7860 – 7863; *Angew. Chem.* **2014**, *126*, 7994 – 7997.

[7] X. Wang, Y. V. Kolen'ko, X. Q. Bao, K. Kovnir, L. Liu, *Angew. Chem. Int. Ed.* **2015**, *54*, 8188 – 8192; *Angew. Chem.* **2015**, *127*, 8306 – 8310.

[8] E. J. Popczun, C. G. Read, C. W. Roske, N. S. Lewis, R. E. Schaak, *Angew. Chem.* **2014**, *126*, 5531 – 5534.

[9] J. Tian, Q. Liu, N. Cheng, A. M. Asiri, X. Sun, *Angew. Chem. Int. Ed.* **2014**, *53*, 9577 – 9581; *Angew. Chem.* **2014**, *126*, 9731 – 9735.

[10] M. Cabán-Acevedo, M. L. Stone, J. Schmidt, J. G. Thomas, Q. Ding, H.-C. Chang, M.-L. Tsai, J.-H. He, S. Jin, *Nat. Mater.* **2015**, *14*, 1245 – 1251.

[11] J. Kibsgaard, T. F. Jaramillo, *Angew. Chem. Int. Ed.* **2014**, *53*, 14433 – 14437; *Angew. Chem.* **2014**, *126*, 14661 – 14665.

[12] F. X. Ma, H. B. Wu, B. Y. Xia, C. Y. Xu, X. W. D. Lou, *Angew. Chem. Int. Ed.* **2015**, *54*, 15395 – 15399; *Angew. Chem.* **2015**, *127*, 15615 – 15619.

[13] S. T. Hunt, T. Nimmanwudipong, Y. Román-Leshkov, *Angew. Chem. Int. Ed.* **2014**, *53*, 5131 – 5136; *Angew. Chem.* **2014**, *126*, 5231 – 5236.

[14] J. K. Nørskov, T. Bligaard, A. Logadottir, J. Kitchin, J. Chen, S. Pandelov, U. Stimming, *J. Electrochem. Soc.* **2005**, *152*, J23 – J26.

[15] M. Johansson, E. Skulason, G. Nielsen, S. Murphy, R. M. Nielsen, I. Chorkendorff, *Surf. Sci.* **2010**, *604*, 718 – 729.

[16] F. A. Al-Odail, A. Anastasopoulos, B. E. Hayden, *Top. Catal.* **2011**, *54*, 77 – 82.

[17] a) B. Behzadian, D. Piron, C. Fan, J. Lessard, *Int. J. Hydrogen Energy* **1991**, *16*, 791 – 796; b) J. Ahmed, P. Trinh, A. M. Mugweru, A. K. Ganguli, *Solid State Sci.* **2011**, *13*, 855 – 861.

[18] A. J. Bard, L. R. Faulkner, *Electrochemical Methods, 2nd ed.*, Wiley, New York, **2001**.

[19] B. Y. Xia, H. B. Wu, X. Wang, X. W. Lou, *J. Am. Chem. Soc.* **2012**, *134*, 13934 – 13937.

[20] T. Cochell, W. Li, A. Manthiram, *J. Phys. Chem. C* **2013**, *117*, 3865 – 3873.

[21] D. M. Jones, E. Owen, *Proc. Phys. Soc. London Sect. B* **1954**, *67*, 297.

[22] S. Kukunuri, P. M. Austeria, S. Sampath, *Chem. Commun.* **2016**, *52*, 206 – 209.

[23] J. M. McEnaney, R. E. Schaak, *Inorg. Chem.* **2015**, *54*, 707 – 709.

[24] a) X. Zou, X. Huang, A. Goswami, R. Silva, B. R. Sathe, E. Mikmeková, T. Asefa, *Angew. Chem.* **2014**, *126*, 4461 – 4465; b) Q. Li, W. Cui, J. Tian, Z. Xing, Q. Liu, W. Xing, A. M. Asiri, X. Sun, *ChemSusChem* **2015**, *8*, 2487 – 2491.

[25] a) Y. Shi, S. Yin, Y. Ma, D. Lu, Y. Chen, Y. Tang, T. Lu, *J. Power Sources* **2014**, *246*, 356 – 360; b) Y.-H. Chung, S. J. Kim, D. Y. Chung, H. Y. Park, Y.-E. Sung, S. J. Yoo, J. H. Jang, *Chem. Commun.* **2015**, *51*, 2968 – 2971; c) D. Strmcnik, M. Escudero-Escribano, K. Kodama, V. R. Stamenkovic, A. Cuesta, N. M. Marković, *Nat. Chem.* **2010**, *2*, 880 – 885.

[26] a) S. Koh, P. Strasser, *J. Am. Chem. Soc.* **2007**, *129*, 12624 – 12625; b) P. Mani, R. Srivastava, P. Strasser, *J. Phys. Chem. C* **2008**, *112*, 2770 – 2778; c) R. Yang, W. Bian, P. Strasser, M. F. Toney, *J. Power Sources* **2013**, *222*, 169 – 176.

[27] a) W. F. Chen, K. Sasaki, C. Ma, A. I. Frenkel, N. Marinkovic, J. T. Muckerman, Y. Zhu, R. R. Adzic, *Angew. Chem. Int. Ed.* **2012**, *51*, 6131 – 6135; *Angew. Chem.* **2012**, *124*, 6235 – 6239; b) N. Markovic, B. Grgur, P. Ross, *J. Phys. Chem. B* **1997**, *101*, 5405 – 5413.

[28] M. Mahmoud, F. Saira, M. El-Sayed, *Nano Lett.* **2010**, *10*, 3764 – 3769.
[29] J. R. McKone, B. F. Sadtler, C. A. Werlang, N. S. Lewis, H. B. Gray, *ACS Catal.* **2013**, *3*, 166 – 169.
[30] B. Hammer, J. K. Nørskov, *Adv. Catal.* **2000**, *45*, 71 – 129.
[31] a) A. Ruban, B. r. Hammer, P. Stoltze, H. L. Skriver, J. K. Nørskov, *J. Mol. Catal. A* **1997**, *115*, 421 – 429; b) B. Hammer, J. Nørskov, *Surf. Sci.* **1995**, *343*, 211 – 220; c) T. Bligaard, J. Nørskov, S. Dahl, J. Matthiesen, C. Christensen, J. Sehested, *J. Catal.* **2004**, *224*, 206 – 217.

Received: August 8, 2016
Revised: August 9, 2016
Published online on ■■ ■■, 0000

A little less gives a lot more: $PdCu_3$ nanoparticles (NPs) are synthesized using a solvothermal method with oleylamine as the solvent, stabilizer, and reducing agent. Electrochemical dealloying transforms $PdCu_3$ NPs into Cu-deficient $PdCu_{3-x}$, which shows enhanced hydrogen evolution reaction activity equivalent to state-of-the-art Pt/C.

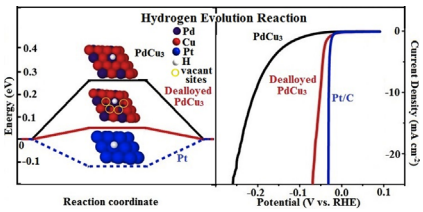

*R. Jana, A. Bhim, P. Bothra, S. K. Pati, S. C. Peter**

■■ – ■■

Electrochemical Dealloying of $PdCu_3$ Nanoparticles to Achieve Pt-like Activity for the Hydrogen Evolution Reaction